Inorganic Chemistry

Article

pubs.acs.org/IC

p-Carborane-Bridged Bipyridine Ligands for Energy Transfer between Two Iridium Centers

M. Teresa Indelli,*[,†] Thomas Bura,[‡] and Raymond Ziessel*[,‡]

[†]Dipartimento di Chimica, Università di Ferrara, INSTM Sezione di Ferrara, 44100 Ferrara, Italy

[‡]Laboratoire de Chimie Organique et Spectroscopies Avancées (ICEEPS-LCOSA), UMR 7515 au CNRS, Ecole Européenne de Chimie, Polymères et Matériaux, Université de Strasbourg, 25 rue Becquerel, 67087 Strasbourg Cedex 02, France

Supporting Information

ABSTRACT: Two iridium(III) complexes displaying for one a high HOMO−LUMO gap and for the other a weaker gap were linked in a controlled and logical manner to closo-*p*-carborane spacers. The bridging ligand is composed of 5-ethynyl-2,2′-bipyridine units, and the peripherical Ir-ligands are orthometalated 2′,4′-difluoro-2-phenylpyridine (dfppy) (λ_{abs} at 400 nm for the "Ir(dfppy)$_2$(bpy′)") for the energy donor fragment and dibenzo[*a*,*c*]phenazine (dbpz) (λ_{abs} at 525 nm for "Ir(dbpz)$_2$(bpy′)") for the energy acceptor fragment. Redox, spectroscopic, and photophysical properties for models and the donor−carborane−acceptor complex were determined. Efficient energy transfer from the "Ir(dfppy)$_2$(bpy′)" moiety to the "Ir(dbpz)$_2$(bpy′)" fragment is occurring with a rate constant of 3.3×10^8 s^{-1} despite weak electronic coupling through the inert *p*-carborane spacer. From flash photolysis experiments it is shown that, by excitation of the donor, a low lying triplet state localized on the acceptor bridging ligand side is formed which decays by conversion to the ^{3}MLCT of the acceptor fragment which phosphoresces at 644 nm.

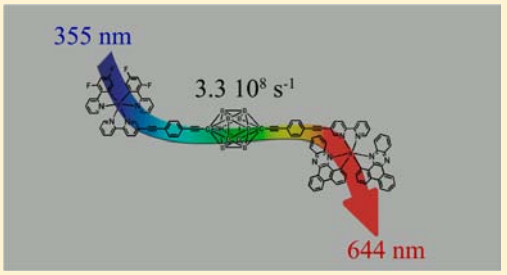

INTRODUCTION

Designing and powering synthetic methodologies for the construction of rigid multisite ligands in which weak electronic interactions are effective represent major challenges and opportunities. Considerable efforts have been devoted to the preparation of ligands and transition metal complexes in order to quantify the level of interaction using spectroscopic tools.[1−3] Multichromophoric systems have been designed and scrutinized with the viewpoint of collecting, transferring, and converting solar energy into useful energy source.[4,5] In the design of such systems the bridging ligands are crucial not only from the structural viewpoint but also for the electronic coupling between the separated subunits.[6] Along these lines, polypyridine transition metal complexes have been largely employed due to their rich photophysics and long-lived triplet excited states that can act as energy donors or energy acceptors for fast and efficient energy transfer processes.[7]

Particularly attractive are molecular systems where photoinduced energy or electron transfer processes can be realized over large distances and in a preferred direction.[8,9] Earlier discoveries have shown that the nature of the spacing units separating photoactive terminals plays a crucial role in the efficiency and mechanism of information transfer.[10,11] Unsaturated systems have been explored and appear to be the most attractive. Among these systems, p-phenylenevinylene oligomers,[12] polyenes,[13,14] polyalkynes,[15−19] polyphenylenes,[20−24] polyphenyl/alkyne,[25,26] and polythiophene[27−29] units have been extensively studied due to their chemical stability and synthetic accessibility.[3,30] Generally, the chemistry required to construct and purify such molecular objects is highly demanding, and up-to-now very few applications have been foreseen. The role of the bridging ligands that anchors the chromophores is usually not innocent because it will not only control the spatial arrangement of the chromophores, and consequently the intercomponent distances and angles, but also influence the electronic communication between the partners.[31,32] In some cases the bridging ligands can participate to the energy transfer processes and can promote cascade energy transfer events over large distances.[33]

Rigid rodlike spacers are attractive building blocks for the construction of supramolecular arrays. For instance, carboranes have been extensively used as templates for the preparation of soft matter,[34] polymers,[35] nonlinear materials,[36] rigid rods,[37] self-assembled molecular structures,[38] and supramolecular species containing carborane derivatives assembled through appropriate metal centers.[31,39] Their derivatives such as metallacarboranes are analogues of metallocenes[40] and, like them, find applications, for example, in medicinal chemistry.[41] Carboranes of the closo form, such as 1,12-dicarbadecaborane ($C_2B_{10}H_{12}$), are geometrically rigid species with an electronic structure making them chemically and thermodynamically very robust. Furthermore, they are transparent to visible and UV light down to about 200 nm and do not exhibit redox activity in standard windows.[42] These properties prompted us to use *closo*-1,12-dicarbadecaborane as a platform to link organic chromophores in a rodlike manner and promote through space Förster resonance energy transfer (FRET).[43]

In a single case, *para*-carborane has been used as a bridging unit between two phosphorescent ruthenium-trisbipyridine units.[44] Mixed valence homometallic complexes have been investigated, and

Received: October 11, 2012
Published: March 7, 2013

   dx.doi.org/10.1021/ic302222q | Inorg. Chem. 2013, 52, 2918−2926

Chart 1

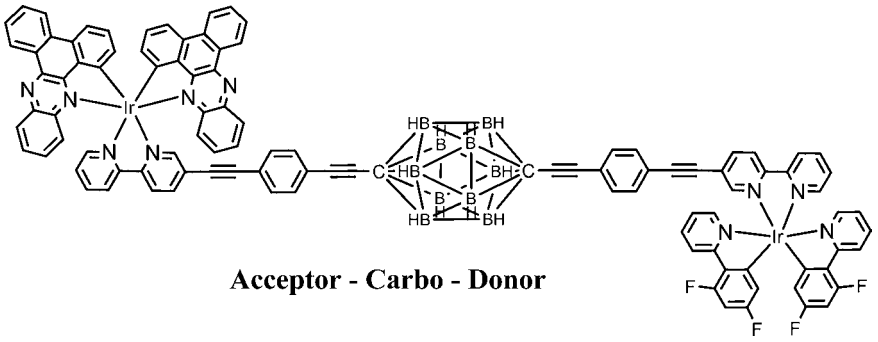

little delocalization through the bridge has been evidenced. However photoinduced electron transfer in mixed valence complexes highlights the effectiveness of such processes. Up to now, no energy transfer between two dissimilar complexes bridged by carborane scaffoldings has been investigated. Within this context we devise a synthetic protocol capable to control by a convergent procedure the construction of donor-bridge-acceptor system bridged by a bipy-Carbo-bipy framework (bipy accounts for 5-ethynyl-2,2′-bipyridine and Carbo for *closo*-p-carborane) and capable to promote electronic energy transfer between two remote cationic Ir(III) centers having dissimilar energy levels of the lowest excited states (Chart 1).

EXPERIMENTAL SECTION

Synthesis and Characterization. *Compound 1.* To a degazed solution of A (47.1 mg, 0.077 mmol) and 5-ethynyl-2,2′-bipyridine (13.9 mg, 0.077 mmol) in benzene (5 mL) and triethylamine (1.5 mL) was added $Pd(PPh_3)_4$ (8.9 mg, 0.008 mmol). The resulting mixture was stirred over a weekend at 60 °C under argon. It was then cooled down to RT (room temperature), dissolved in CH_2Cl_2, washed with water, and extracted with dichloromethane. Organic layers were dried over Na_2SO_4 and evaporated under vacuum. The product was purified by silica gel chromatography (from 5/95 to 10/90 ethyle acetate/petroleum ether) to obtain 46.2 mg (90%) of compound **1**. ^{1}H NMR (200 MHz, $CDCl_3$) δ (ppm): 0.66 (q, 6 H, ^3J = 7.8 Hz), 1.03 (t, 9 H, ^3J = 7.9 Hz), 7.18−7.39 (m overlapping with slovent, 7 H), 7.42 (d, 2H, ^3J = 8 Hz), 7.75−7.97 (m, 2 H), 8.41 (d, 2 H, ^3J = 8.2 Hz), 8.61−8.87 (m, 2 H).

Compound 2. In the round-bottom flask with THF (5 mL) and MeOH (1 mL) was added compound **1** (45 mg, 0.068 mmol) and NaOH (14 mg, 0.34 mmol). The reaction was agitated during 1 h at RT. Then, the solvent was evaporated to dryness. The crude material was purified by column chromatography on alumina eluted with a mixture of CH_2Cl_2/petroleum ether (40/60) and afforded compound **2** as a white powder (35 mg, 95%).

^{1}H NMR ($CDCl_3$, 300 MHz): 1.63−3.15 (broad B−H absorption 10H), 3.17 (s, 1H), 7.25−7.40 (m, 7H), 7.47 (d, 2H ^3J = 8.2 Hz), 7.81−7.94 (m, 2H), 8.42 (d, 2H, ^3J = 7.9 Hz), 8.69−8.80 (m, 2H). EI-MS 546.2 ([M] 100). Anal. Calcd for $C_{32}H_{26}B_{10}N_2$ (Mr = 546.67): C, 70.31; H, 4.79 ; N, 5.12. Found: C, 70.20; H, 4.52; N, 4.88.

Compound 5. The dimeric complex **3** (100 mg, 0.084 mmol) was dissolved in dichloromethane (6 mL) and methanol (6 mL), and 5-bromo-2,2′-bipyridine (42 mg, 0.176 mmol) was added as a solid. The mixture was heated at 60 °C during the night. The solution was cooled down to RT and the solvent evaporated to dryness. The residue was dissolved in DMF (1 mL) and was added dropwise through a pad of Celite into an aqueous solution of KPF_6 (500 mg in 20 mL of water). The precipitate was collected on paper and washed with water (3 × 100 mL). The complex was dried in air and purified by column chromatography on alumina. The desired complex (yellow band) was eluted with a gradient of methanol (0−1%) in dichloromethane as mobile phase. The analytically pure complex **5** was obtained as yellow powder by crystallization in a mixture dichloromethane/diethylether (160 mg, 87%).

^{1}H NMR ($(CD_3)_2CO$, 300 MHz): 5.76 (dd, 1H ^3J = 8.6 Hz, ^4J = 2.85 Hz), 5.84 (dd, 1H ^3J = 8.4 Hz, ^4J = 2.30 Hz), 6.70−6.79 (m, 2H), 7.21−7.28 (m, 2H), 7.74−7.78 (m, 1H), 7.91−7.95 (m, 1H), 8.04−8.10 (m, 3H), 8.19−8.22 (m, 2H), 8.31−8.40 (m, 3H), 8.50−8.53 (m, 1H), 8.80−8.88 (m, 2H). EI-MS *m*/*z* 809.0 ($[M - PF_6]^+$ 100); 807.0 ($[M - PF_6]^+$ 100). Anal. Calcd for $C_{32}H_{19}BrF_4IrN_4(PF_6)$ (Mr = 952.6): C, 40.35; H, 2.01; N, 5.88. Found: C, 40.11; H, 1.87; N, 5.67.

Compound 6. In a Schlenk tube compound **2** (40 mg, 0.073 mmol) and complex **5** (69 mg, 0.073 mmol) were dissolved in a mixture of benzene (5 mL), CH_3CN (5 mL), and triethylamine (2 mL). Argon was bubbled through the mixture for 30 min, then $[Pd(PPh_3)_4]$ (9 mg) was added, and the mixture was stirred at 65 °C for 36 h. The solution was cooled down to RT and the solvent evaporated to dryness. The residue was dissolved in DMF (1 mL) and was added dropwise through a pad of Celite into an aqueous solution of KPF_6 (500 mg in 20 mL of water). The precipitate was collected on paper and washed with water (3 × 50 mL). The complex was dried in air and was purified by column chromatography on alumina. The desired complex was eluted with a gradient of methanol (0−1%) in dichloromethane as mobile phase. The analytically pure complex **6** was obtained as yellow powder by hot crystallization in acetone (70 mg, 68%).

^{1}H NMR ($(CD_3)_2CO$, 300 MHz): 1.63−3.15 (broad B−H absorption overlapping with H_2O), 5.76 (dd, 1H ^3J = 8.6 Hz, ^4J = 2.31 Hz), 5.82 (dd, 1H ^3J = 8.6 Hz, ^4J = 2.31 Hz), 6.73−6.81 (m, 2H), 7.23−7.27 (m, 2H), 7.41−7.49 (m, 7H), 7.59−7.61 (m, 2H), 7.75−7.79 (m, 1H), 7.91−7.98 (m, 2H), 8.05−8.10 (m, 4H), 8.22−8.28 (m, 2H), 8.34−8.54 (m, 6H), 8.69−8.70 (m, 1H), 8.82 (s broad, 1H), 8.89−8.94 (m, 2H). EI-MS *m*/*z* 1273.4 ($[M - (PF_6)]^+$ 100). Anal. Calcd for $C_{64}H_{44}B_{10}F_4IrN_6(PF_6)$ (Mr = 1418.36): C, 54.20; H, 3.13; N, 5.93. Found: C, 54.08; H, 3.25; N, 5.77.

Compound 8. The dimeric complex 7 (84 mg, 0.054 mmol) and 5-ethynyl-2,2′-bipyridine (20 mg, 0.088 mmol) were dissolved in dichloromethane (6 mL) and methanol (6 mL). The mixture was heated at 60 °C during the night. The solution was cooled down to RT and the solvent evaporated to dryness. The residue was dissolved in DMF (1 mL) and was added dropwise through a pad of Celite into an aqueous solution of KPF_6 (500 mg in 20 mL of water). The precipitate was collected on paper and washed with water (3 × 100 mL). The complex was dried in air and was purified by column chromatography on alumina. The desired complex was eluted with a gradient of methanol (0−1%) in dichloromethane as mobile phase. The analytically pure complex **8** was obtained as orange powder by crystallization in a mixture dichloromethane/diethylether (20 mg, 35%).

^{1}H NMR ($CD_3)_2CO$, 300 MHz): 3.95 (s, 1H), 6.62 (d, 1H, ^3J = 7.6 Hz), 6.73 (d, 1H, ^3J = 7.6 Hz), 7.12−7.21 (m, 2H), 7.44−7.57 (m, 5H), 7.78−8.01 (m, 6H), 8.11−8.24 (m, 4H), 8.32 (t, 2H, ^3J = 7.9 Hz), 8.43 (d, 2H, ^3J = 8.6 Hz), 8.68 (d, 2H, ^3J = 8.6 Hz), 8.73−8.77 (m, 2H), 9.39−9.43 (m, 2H). EI-MS *m*/*z* 931.4 ($[M - PF_6]^+$ 100). Anal. Calcd for $C_{52}H_{30}IrN_6(PF_6)$ (Mr = 1076.02): C, 58.04; H, 2.81; N, 7.81. Found: C, 58.12; H, 3.04; N, 7.62.

Compound [Ir(dfppy)$_2$-Carbo-Ir(dfppy)$_2$](PF$_6$)$_2$. The dimeric complex **3** (12.2 mg, 0.0103 mmol) and compound **6** (29 mg, 0.0206 mmol)

dx.doi.org/10.1021/ic302222q | *Inorg. Chem.* 2013, 52, 2918−2926

Scheme 1

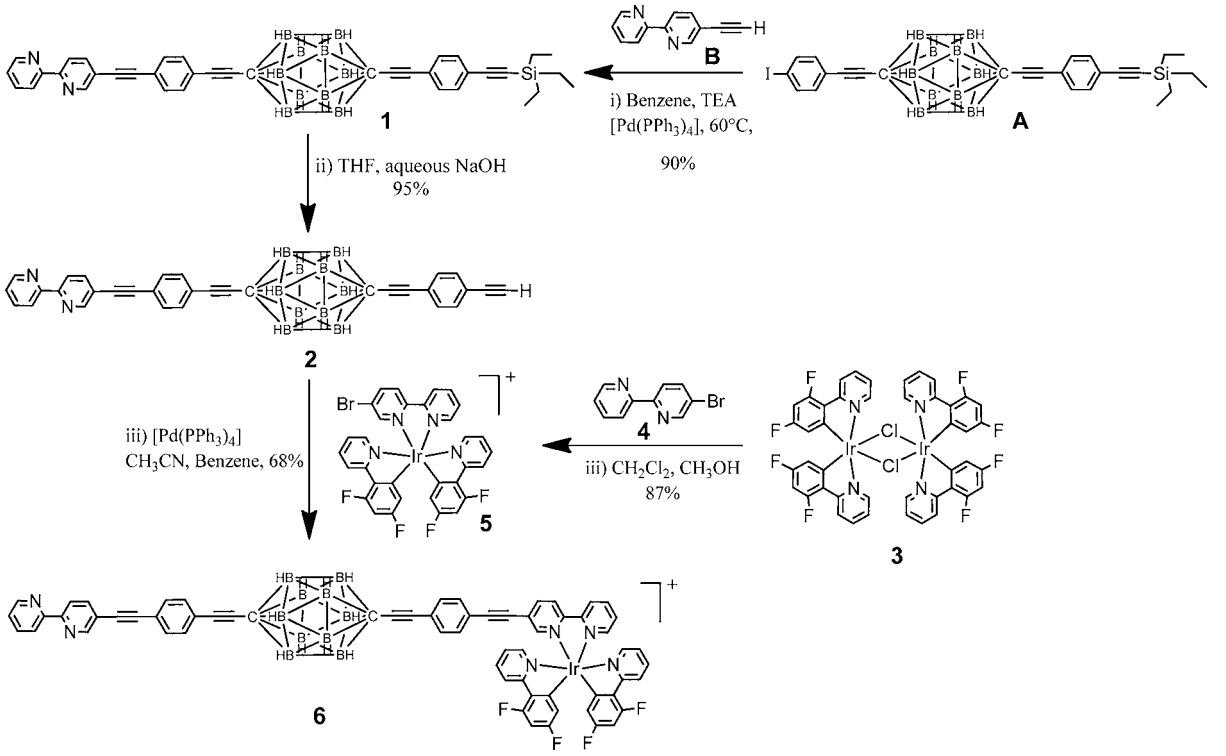

Scheme 2

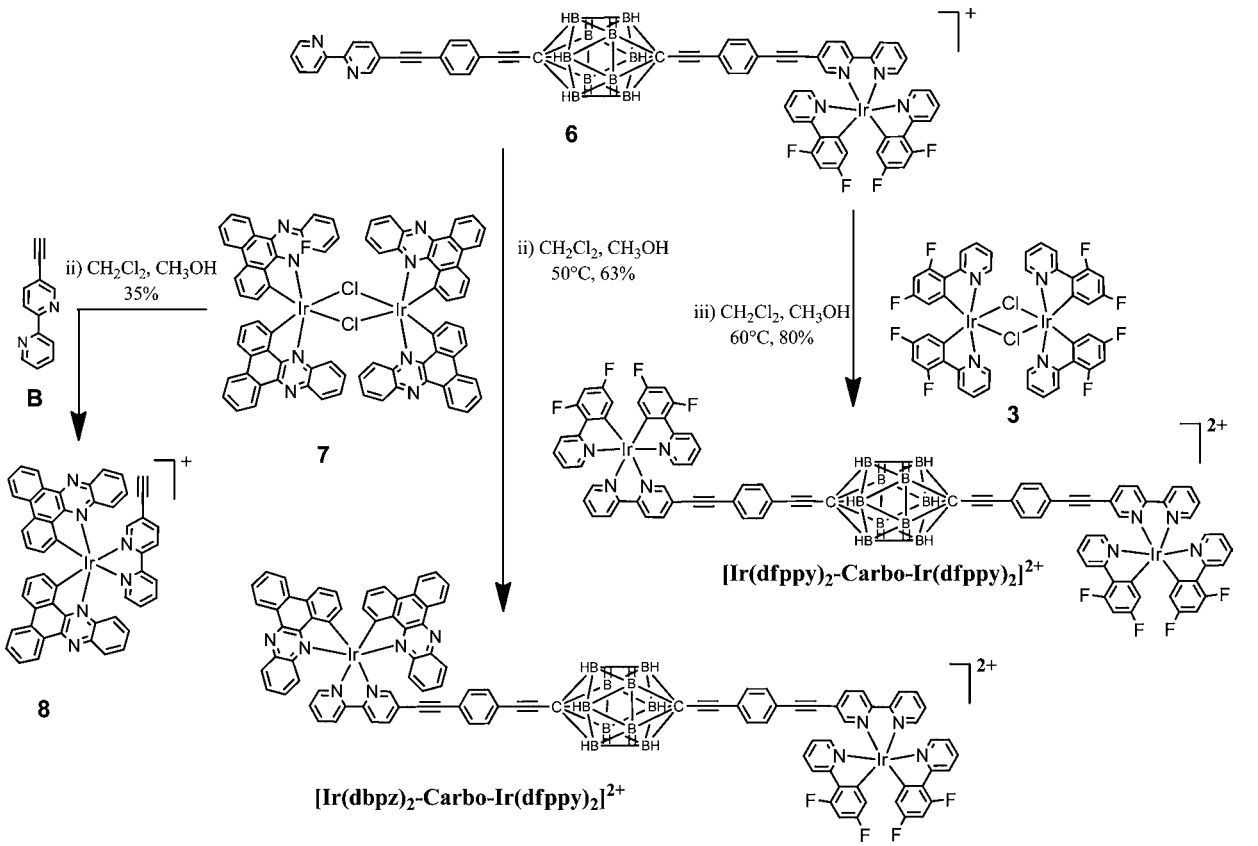

were dissolved in dichloromethane (4 mL) and methanol (4 mL). The mixture was heated at 60 °C during the night. The solution was cooled down to RT and the solvent evaporated to dryness. The residue was dissolved in DMF (1 mL) and was added dropwise through a pad of Celite into an aqueous solution of KPF_6 (500 mg in 20 mL water). The precipitate was collected on paper and washed with water (3 ×

dx.doi.org/10.1021/ic302222q | Inorg. Chem. 2013, 52, 2918−2926

100 mL). The complex was dried in air and was purified by column chromatography on alumina. The desired complex was eluted with a gradient of methanol (0−3%) in dichloromethane as mobile phase. The analytically pure compound $[Ir(dfppy)_2\text{-Carbo-}Ir(dfppy)_2](PF_6)_2$ was obtained as yellow powder by hot crystallization in acetone (35 mg, 80%).

^{1}H NMR ($CDCl_3$, 400 MHz): 2.01−3.30 (broad B−H absorption 10H) 5.65 (dd, 2H ^3J = 8.2 Hz, ^4J = 2.04 Hz), 5.70 (dd, 2H ^3J = 8.6 Hz, ^4J = 2.4 Hz), 6.54−6.61 (m, 4H), 7.11−7.14 (m, 4H), 7.29 (d, 4H, ^3J = 8.2 Hz), 7.39 (d, 4H, ^3J = 8.2 Hz), 7.49−7.56 (m, 6H), 7.81−7.85 (m, 4H), 7.91−7.94 (m, 4H), 8.18−8.24 (m, 4H), 8.30−8.35 (m, 4H), 8.67−8.72 (m, 4H). EI-MS m/z 1990.9 ($[M - (PF_6)]^+$ 100). Anal. Calcd for $C_{86}H_{56}B_{10}F_8Ir_2N_8(PF_6)_2$ (Mr = 2135.88): C, 48.36; H, 2.64; N, 5.25. Found: C, 48.59; H, 2.77; N, 5.02.

Compound [Ir(dbpz)$_2$-Carbo-Ir(dfppy)$_2$](PF$_6$)$_2$. The dimeric complex 7 (30 mg, 0.0170 mmol) and compound **6** (24 mg, 0.170 mmol) were dissolved in dichloromethane (4 mL) and methanol (4 mL). The mixture was heated at 60 °C during the night. The solution was cooled down to RT and the solvent evaporated to dryness. The residue was dissolved in DMF (1 mL) and dropwise added through a pad of Celite into an aqueous solution of KPF_6 (500 mg in 20 mL water). The precipitate was collected on paper and washed with water (3 × 100 mL). The complex was dried in air and was purified by column chromatography on alumina. The desired complex was eluted with a gradient of methanol (0−2%) in dichloromethane as mobile phase. The analytically pure compound $[Ir(dbpz)_2\text{-Carbo-}Ir(dfppy)_2](PF_6)_2$ was obtained as orange powder by crystallization in a mixture CH_3CN/Et_2O (25 mg, 63%). ^{1}H NMR ($(CD_3)_2CO$, 300 MHz): 1.63−3.15 (broad B−H absorption overlapping with H_2O), 5.76 (dd, 1H ^3J = 8.6 Hz, ^4J = 2.00 Hz), 5.82 (dd, 1H ^3J = 8.6 Hz, ^4J = 2.31 Hz), 6.68−6.80 (m, 4H), 7.10−7.33 (m, 8H), 7.40−7.57 (m, 6H), 7.73−7.78 (m, 2H), 7.81−7.93 (m, 5H), 7.97−8.09 (m, 6H), 8.13−8.27 (m, 7H), 8.32−8.45 (m, 8H), 8.66−8.68 (m, 2H), 8.75−8.93 (m, 4H), 9.38−9.43 (m, 2H). EI-MS m/z 2169.2 ($[M - (PF_6)]^+$ 100). Anal. Calcd for $C_{104}H_{66}B_{10}F_4Ir_2N_{10}(PF_6)_2$ (Mr = 2314.17): C, 53.98; H, 2.87; N, 6.05. Found: C, 54.19; H, 3.07; N, 5.84.

RESULTS AND DISCUSSION

Synthesis. The preparations of the target $[Ir(dbpz)_2\text{-Carbo-}Ir(dfppy)_2](PF_6)_2$ and reference complexes are sketched in Schemes 1 and 2. The synthesis of the pivotal starting material **A** bearing one protected alkyne function and a reactive iodophenyl fragment has been previously described.[45] Cross-coupling **A** with 5-ethynyl-2,2′-bipyridine **B**[46] produces ligand **1** in excellent yield. This molecule is easily deprotected under basic conditions to provide the terminal alkyne **2** in good yields. Cross-coupling complex **5** bearing a reactive bromo-aryl function with ligand **2** provides the cationic iridium complex **6**. The key precursor **5** was prepared as a single isomer from the neutral dimer **3** and 5-bromo-2,2′-bipyridine **4** (Scheme 1).[47] The use of 2′,4′-difluoro-2-phenylpyridine (dfppy) allows us to prepare pale yellow complexes displaying optical transitions at about 400 nm.[48]

With complex **6** in hand it was possible to chelate the free bipyridine residue with a second iridium center by reacting **6** with dimer **7** under standard conditions providing the dicationic $[Ir(dbpz)_2\text{-Carbo-}Ir(dfppy)_2]^{2+}$ in good yields (Scheme 2). The use of dibenzo[*a*,*c*]phenazine (dbpz) allows us to prepare deep red complexes displaying optical transitions above 530 nm.[49] On the other hand the preparations of the donor and acceptor complexes that are useful for the spectroscopic measurements were completed as depicted in Scheme 2. The acceptor complex **8** was easily prepared by reacting the dimer **7** with ligand **B** and the acceptor complex $[Ir(dfppy)_2\text{-Carbo-}Ir(dfppy)_2]^{2+}$ (**D**) by reacting the mononuclear complex **6** with dimer **3**. For all charged complexes the counteranion is hexafluorophosphate which facilitates the purification by column chromatography. The molecular structures of the intermediates and final compounds were unambiguously assigned by NMR, ESI-MS, and optical measurements.

Absorption Spectra. The compound studied is made of two different chromophoric units, $Ir(dbpz)_2$- and $Ir(dfppy)_2$-bridged by a *p*-carborane-containing ligand (Carbo). In order to discuss the photophysical and electrochemical results obtained for the bichromophoric complex, it is useful to study simple compounds that model the intrinsic behavior of the individual chromophoric units. For $Ir(dfppy)_2$-unit, an appropriate model is represented by the binuclear $[Ir(dfppy)_2\text{-Carbo-}Ir(dfppy)_2]^{2+}$ complex, whereas for $Ir(dbpz)_2$-unit, the mononuclear $[Ir(dbpz)_2(bpy')]^+$ complex **8** is available as model.

The spectroscopic, photophysical, and redox properties of the bichromophoric complex were investigated in CH_2Cl_2 solution and compared to those of the model compounds. The absorption spectra of the model compounds are shown in Figure 1.

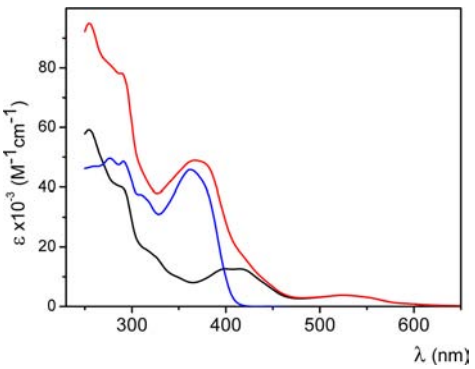

Figure 1. Absorption spectra of $[Ir(dfppy)_2\text{-Carbo-}Ir(dfppy)_2]^{2+}$, donor model (×$^1/_2$, blue line); $[Ir(dppz)_2(bpy')]^+$, acceptor model (black line); and $[Ir(dfppy)_2\text{-Carbo-}Ir(dbpz)_2]^{2+}$ bichromophoric complex (red line) in CH_2Cl_2 solution at room temperature.

In the spectrum of $[Ir(dbpz)_2(bpy')]^+$, beside the ligand centered (LC) bands in the UV region, there are two bands in the visible region at 410 and 525 nm, which can be assigned as metal to ligand charge transfer MLCT transitions, localized on the bpy-based ligand (higher energy band) and on the cyclometalating dbpz ligands (lower energy band), respectively. These assignments are supported by redox results that show that the extended aromatic dbpz ligand is easier to reduce than the bpy-based ligand (vide infra). On the other hand, the binuclear $[Ir(dfppy)_2\text{-Carbo-}Ir(dfppy)_2]^{2+}$ complex does not absorbs in the visible (Figure 1), showing intense bands in the UV region due to the ligand centered (LC) transitions (possibly overlapping less intense metal to ligand charge transfer, MLCT bands). The spectrum of bichromophoric complex, $[Ir(dfppy)_2\text{-Carbo-}Ir(dbpz)_2]^{2+}$, shown in Figure 1, clearly exhibits the typical absorptions of both the $Ir(dbpz)_2$- and $Ir(dfppy)_2$-units. The substantial additivity of the spectroscopic properties of the molecular components in the complex points toward an absence of extensive electronic delocalization across the bridging ligand[38−44] and warrants a localized description of the system studied.[6] Figure 1 shows that fully selective excitation of the $Ir(dbpz)_2$-unit can be achieved at wavelength longer than 500 nm, whereas the $Ir(dfppy)_2$-unit can be excited only partially (e.g., 60% at 355 nm). For the roles that they play in the photophysical experiments described below, the $Ir(dfppy)_2$- and $Ir(dbpz)_2$-units are thereafter denoted, respectively, as the donor and acceptor units.

dx.doi.org/10.1021/ic302222q | Inorg. Chem. 2013, 52, 2918−2926

Redox Properties. The electrochemical properties of the bichromophoric complex were examined by cyclic voltammetry in dichloromethane solution (electrochemical window from +1.6 to −2.2 V, $TBAPF_6$ 0.1 M supporting electrolyte, Pt microdisk working electrode, SCE reference electrode, silver wire counterelectrode). For purposes of comparison, the electrochemical behavior of the model compounds was studied under the same experimental conditions (Figure 2). The results are reported in Table 1.

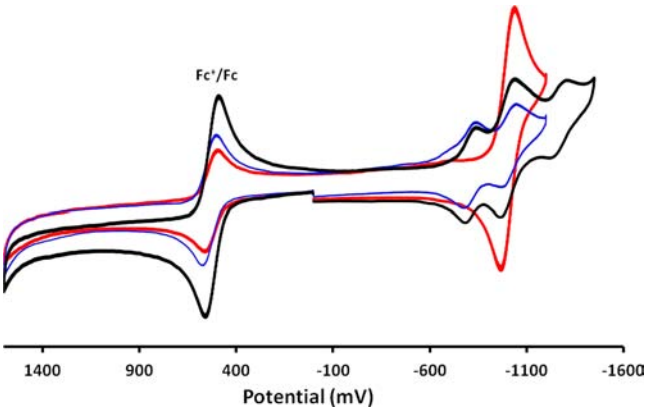

Figure 2. Cyclic voltammogram of 0.5 mM: (blue trace) complex **8**; (red trace) complex **5**; (black trace) binuclear complex $[Ir(dfppy)_2$-Carbo-$Ir(dbpz)_2]^{2+}$ in dichloromethane with 0.1 M $TBAPF_6$. Working electrode, Pt disk; counterelectrode, Pt coil; reference electrode, SCE. Scan rate was 0.2 V/s.

Table 1. Redox Potentials of the Bichromophoric Complex and of the Model Compounds[a]

complex	E°_{red}, V ($E_p^a - E_p^c$, mV)
$[Ir(dfppy)_2$-Carbo-$Ir(dfppy)_2]^{2+}$	−1.12 (65);[b] −1.75 (irr)[b]
$[Ir(dbpz)_2(bpy')]^+$	- 0.96 (60); −1.17 (60); −1.50 (60)
$[Ir(dfppy)_2$-Carbo-$Ir(dbpz)_2]^{2+}$	−0.95 (60); −1.14 (70);[b] −1.41 (70); −1.55 (irr); −1.76 (irr); 1.95 (irr)

[a] CH_2Cl_2 solution with 0.1 M $TBAPF_6$. Potential values vs SCE, values calculated as average of the cathodic and anodic peaks, one-electron process unless otherwise noted. [b] Two-electron process.

In the anodic region (0 to +1.6 V vs SCE) the complexes are not active. As usual for Ir(III) complexes with imine ligands,[50] the cathodic region is characterized by ligand centered reduction processes. For the $[Ir(dfppy)_2$-Carbo-$Ir(dfppy)_2]^{2+}$ binuclear donor model, a reversible bielectronic wave is observed at −1.12 V versus SCE. This process can be attributed to reduction of the bpy-like moiety of the bridging ligand by comparison with the redox behavior of related Ir(III) complexes containing ppy cyclometalating and bpy ligands.[51] The bielectronic nature of the reduction process indicates that the two bpy-like moieties of the bridge are reduced simultaneously, again consistent with a weak through-bridge interaction between the two metallic units. A subsequent irreversible wave is observed likely due to reduction of one of the dfppy terminal ligands. The $[Ir(dbpz)_2(bpy')]^+$ acceptor model exhibits three well resolved reversible reduction waves. The first falls at a potential definitely less negative (−0.96 V vs SCE) than that for the first reduction process in the donor model, and, as a consequence, can be safely assigned to reduction of the dbpz ligand. In the more negative region, the reduction of bpy′ ligand occurs at −1.17 V versus SCE, a potential value very close to reduction of bpy-like moiety of the bridge. The third wave can be tentatively assigned to the reduction of the second dbpz ligand. The voltammetric behavior of $[Ir(dfppy)_2$-Carbo-$Ir(dbpz)_2]^{2+}$ bichromophoric complex is a nice combination of the waves observed for the model components confirming a very weak degree of electronic communication between the two moieties through the *p*-carborane bridge and justifying the consideration of the bichromophoric complex as true supramolecular species.[7a]

Emission. Stationary emission measurements were carried out in room temperature fluid solution and in a rigid matrix (EtOH/MeOH 4/1) at 77 K. The relevant emission properties of the systems studied are collected in Table 2. At room temperature, the model complexes as well as the bichromophoric complex give rise to relatively intense emissions ($\Phi = (1-6) \times 10^{-2}$, see Table 2).

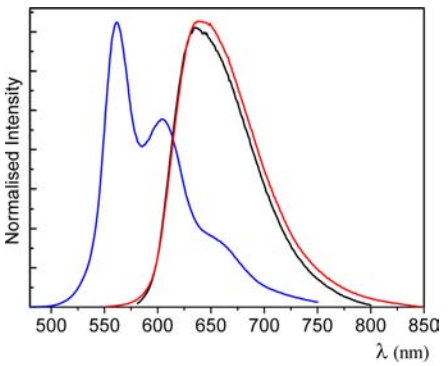

Figure 3. Emission spectra of $[Ir(dfppy)_2$-Carbo-$Ir(dfppy)_2]^{2+}$, donor model (blue line); $[Ir(dbpz)_2(bpy')]^+$, acceptor model (black line); and $[Ir(dfppy)_2$-Carbo-$Ir(dbpz)_2]^{2+}$ bichromophoric complex (red line) in CH_2Cl_2 solution at room temperature.

The emission spectra in room temperature CH_2Cl_2 solution of the bichromophoric complex together with those of the two models are shown in Figure 3. The acceptor model ($[Ir(dbpz)_2(bpy')]^+$) exhibits a broad, structureless band with a maximum at 640 nm. The lifetime of this emission, strongly quenched by

Table 2. Photophysical Properties of the Bichromophoric Complex and of the Model Species

	298 K[a]				77 K[b]		
complex	λ_{em}^{max} (nm)	τ^d (μs)	Φ_{em}^e	k_r^f (s^{-1})	λ_{em}^{max} (nm)	τ (μs)	E^{0-0c} (eV)
$[Ir(dfppy)_2$-Carbo-$Ir(dfppy)_2]^{2+}$	561	3.3	0.015	1.7×10^4	542	30	2.29
$[Ir(dbpz)_2(bpy')]^+$	640	2.0	0.059	7.9×10^4	630	17	1.59
$[Ir(dfppy)_2$-Carbo-$Ir(dbpz)_2]^{2+}$	644	1.7	0.060[f]	8.6×10^4	630	18	1.59

[a] In CH_2Cl_2 solution. [b] In EtOH/MeOH, 4/1, rigid matrix. [c] Obtained from the maximum of the 77 K emission. [d] Deaerated solution. [e] Measured in aerated solution, using $Ru(bpy)_3^{2+}$ as reference. [f] Radiative rate constant, $k_r = \Phi_{em}/\tau_{aer}$; independent of the excitation wavelength.

dx.doi.org/10.1021/ic302222q | Inorg. Chem. 2013, 52, 2918−2926

oxygen, is 2.0 μs in deaerated solution with a strictly monoexponential decay, regardless of monitoring wavelength. The spectral shape, together with the properties reported in Table 2, clearly indicate that the nature of this emission is a phosphorescence from a metal to ligand charge transfer (MLCT) triplet state. In this complex two types of MLCT states are present, one localized on the bpy-like ligand and the other involving the dbpz cyclometalating ligand. On the basis of the spectroscopic (Figure 1) and redox results (Table 1) we can easily assign the emitting state as MLCT triplet localized on the dbpz ligand.

By contrast, the emission of the donor model, $[Ir(dfppy)_2$-Carbo-$Ir(dfppy)_2]^{2+}$, shows different properties with respect the acceptor emission (Figure 3): it is structured with a maximum at 550 nm, a longer lifetime (3.3 μs), and a significantly smaller radiative rate constant (see Table 2). These features clearly suggest that in this complex the emission is a phosphorescence from the lowest ligand centered (LC) triplet localized on the bridging ligand.[52,53]

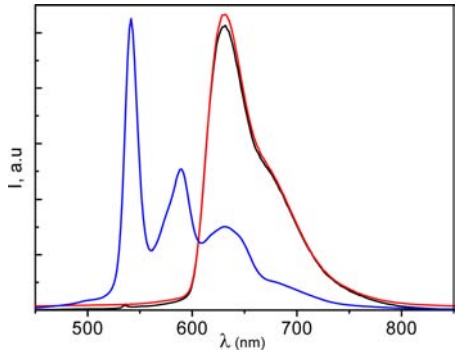

Figure 4. Emission spectra of $[Ir(dfppy)_2$-Carbo-$Ir(dfppy)_2]^{2+}$, donor model (blue line); $[Ir(dbpz)_2(bpy')]^+$, acceptor model (black line); and $[Ir(dfppy)_2$-Carbo-$Ir(dbpz)_2]^{2+}$ bichromophoric complex (red line) in rigid matrix (EtOH/MeOH 4/1) at 77 K.

In a rigid matrix (EtOH/MeOH 4/1) at 77 K, for both model complexes, the emissions become more intense (Figure 4) with shapes and the lifetimes (see Table 2) that confirm the room temperature assignments.

As far as the behavior of the $[Ir(dfppy)_2$-Carbo-$Ir(dbpz)_2]^{2+}$ bichromophoric complex is concerned, a single emission practically identical (spectral region, shape and quantum yield) to that exhibited by the acceptor model appears (Figure 3), regardless of excitation wavelength. In particular, upon substantial excitation of the donor unit (λ = 355 nm), (i) no emission with characteristic features of the donor model is detected, clearly indicating that the emitting state of the donor unit is completely quenched, and (ii) the acceptor emission is efficiently sensitized (as shown by the close correspondence of the excitation spectrum to the absorption spectrum, Figure S8 of Supporting Information). These two results provide strong evidence for the occurrence of an efficient energy transfer process (eq 1):

$$^*\text{Donor–Carbo–Acceptor} \rightarrow \text{Donor–Carbo–Acceptor}^* \quad (1)$$

On the basis of the emitting features of the two chromophoric units, this energy transfer process is quite exergonic. A value of −0.35 eV can be obtained from the energy of the lowest emitting excited states of the two components (see E^{0-0} reported in Table 2). From the excitation spectrum (Figure S8 of Supporting Information) the efficiency of the energy transfer process is estimated to be practically unitary. The fact that, at 77 K, a single emission with the same features as that of the acceptor model is observed (Figure 4 and Table 2) shows that the energy transfer process is efficient even at low temperature.

Time Resolved Transient Emission and Absorption Spectroscopy. In order to investigate the kinetic and the mechanism of the energy transfer process, time-resolved experiments in nanosecond time scale were performed by using laser flash photolysis and single photon counting techniques.

Emission. Time resolved emission experiments on bichromophoric complex solutions were carried out by using nanosecond laser excitation at 355 nm. The emission spectra were measured at different delay times after the laser pulse. All the spectra are identical to the emission spectrum observed in spectrofluorimetric experiments showing the distinctive features of the emission of the acceptor unit. Despite the fact that at the excitation wavelength efficient light absorption by the donor takes place, no donor emission was detected, even with the shortest possible delay (5 ns) after laser excitation. The emission decay was strictly monoexponential with a lifetime of 1.7 μs in deaerated acetonitrile, a value very similar to the lifetime of the model acceptor (Table 2). These results are consistent with the occurrence of an energy transfer process from donor to acceptor unit and, in addition, clearly demonstrate that this process takes place within the laser pulse (8 ns).

In order to evaluate the rate of the energy transfer process, single photon counting experiments were performed by excitation at 380 nm where the light is substantially (50%) absorbed by the donor unit. The emission decay, measured at λ = 550 nm (maximum of the donor emission), is not monoexponential (Figure S9 of Supporting Information). It consists of two components: a major (85%) short-lived component with a lifetime of 3.2 ns and a minor (15%) component with a lifetime >30 ns. The short-lived component maximizes at 550 nm, decreasing in amplitude at shorter and longer wavelengths. This component is assigned to the decay of the donor emission, while the latter one can be easily assigned to long-lived emission from the acceptor unit (not completely negligible at this emission wavelength).[54] From the lifetime of the short-lived component, a value of 3.3×10^8 s^{-1} can be estimated for the rate of the energy transfer process.

As for the mechanism of this process is concerned, two types of mechanisms, Förster-type or Dexter-type, must be considered.[7a] The rate constant for Förster energy transfer can be calculated according to Förster equation[55] which contains the spectroscopic properties of the two molecular components (absorption spectrum of the acceptor, see Figure 1, and emission spectrum of the donor, see Figure 3) with the following appropriate parameters: Φ_D and τ_D (luminescence quantum yield and lifetime of the donor, see Table 2), n (solvent refractive index) = 1.424, k^2 (statistical orientation factor) = $^2/_3$. As far as the donor–acceptor distance is concerned, since the two chromophores are delocalized partly over the bridge, it is difficult to assign an exact value, but a range of distances between a maximum (32.36 Å, Ir–Ir distance) and a minimum value (25.69 Å, Ir–bridge distance) must be taken into consideration in the calculation. The calculations, performed using Photochem CAD,[56] lead to values in the range 1.3×10^5 to 3.4×10^4 s^{-1}, much lower than the experimental value (3.3×10^8 s^{-1}). The Förster mechanism can, therefore, be easily ruled out, and it is reasonable to assume that the Dexter-type mechanism[57] is active in the energy-transfer process.

dx.doi.org/10.1021/ic302222q | Inorg. Chem. 2013, 52, 2918–2926

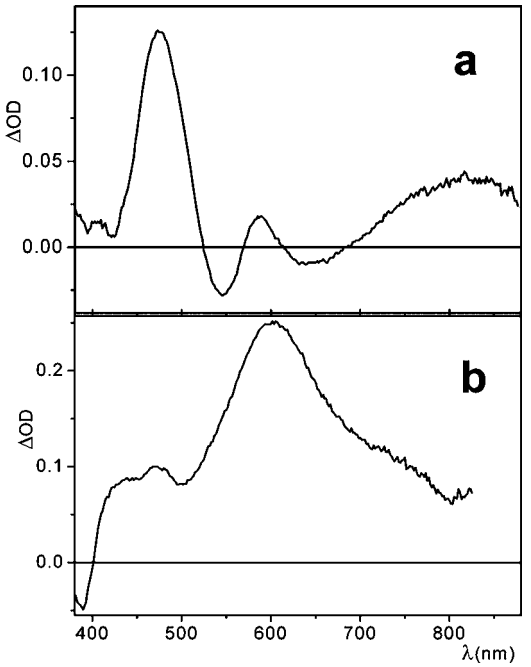

Figure 5. Transient absorption spectrum in CH_2Cl_2 of $[Ir(dbpz)_2(bpy')]^+$, acceptor model (a) and of $[Ir(dfppy)_2\text{-Carbo-}Ir(dfppy)_2]^{2+}$, donor model (b) taken immediately after laser pulse (λ_{exc} = 355 nm; half-width = 8 ns) in CH_2Cl_2 solution at room temperature.

Absorption. The transient absorption spectra obtained in the laser photolysis (λ_{exc} = 355 nm) of the model complexes are shown in Figure 5a,b.

The transient observed for the acceptor model shows the typical features of the absorption spectrum of a MLCT state:[58] (i) positive absorptions (a strong, sharp absorption band at 475 nm and a weaker broad absorption in the 600−850 nm region) characteristic of the formation of a ligand radical anion, and (ii) bleaching at 550 nm that corresponds very closely to the ground-state absorption and an apparent bleaching around 650 nm due to emission. The transient decay was strictly monoexponential and matches well the emission decay, indicating that the transient spectrum is associated with the emissive MLCT charge transfer triplet state localized on the dbpz ligand.

The transient spectrum of the binuclear donor model (Figure 5b) fully differs from that observed for the acceptor model. It is dominated by an intense broad absorption band at 600 nm. In addition, a bleaching corresponding to the ground state absorption appears in the near UV region, and an apparent bleaching due to emission is observed at 560 nm. The decay is monoexponential with the same lifetime as emission confirming that the transient is associated to the LC emitting state localized on the bridging ligand.

Laser flash photolysis of the bichromophoric complex was carried out using 355 nm as excitation wavelength, which corresponds to the absorption by the bridging ligand. In Figure 6 the transient spectra, measured at different delay times after the laser pulse, are reported.

The important result is that, for this system, unlike the case of the model complexes, the shape of the transient observed was found to be time dependent. The spectrum measured immediately after the laser pulse (5 ns delay time) shows an positive absorption in the whole region investigated (400−850 nm) dominated by two intense bands peaking at 472 and 575 nm

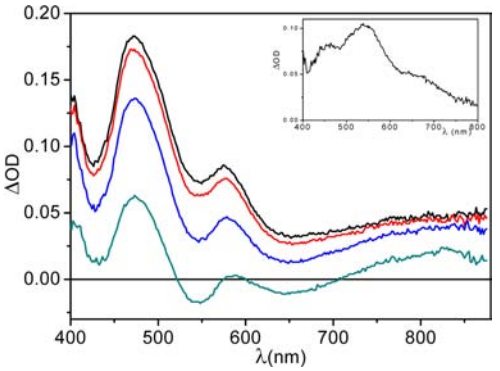

Figure 6. Transient absorption spectra in CH_2Cl_2 of $[Ir(dfppy)_2\text{-Carbo-}Ir(dbpz)_2]^{2+}$ bichromophoric complex, measured at different delay times (5 ns, black; 10 ns, red line; 50 ns, blue line; 300 ns, green line) after the laser pulse (λ_{exc} = 355 nm; half-width = 8 ns). Inset shows spectrum obtained by subtraction of the trace measured at 300 ns delay time from the initial trace.

and a weak broad band around 600 nm. On a longer time scale (300 ns delay time), the absorption at 575 nm practically disappears and the transient evolves to a spectrum identical to the excited state spectrum of the model acceptor (Figure 5a). The decay of the transient absorption is clearly not exponential and consists of two components, a short component with a lifetime of ca. 100 ns and a long component with a lifetime of 1.6 μs, a value very similar to the emission lifetime. The relative amplitudes of the two components are strongly wavelength-dependent: at 550 nm the short component is predominant (ca. 80%) whereas at 475 nm it is practically negligible (ca. 10%). On the basis of the lifetime and spectral features, the long-lived transient can be assigned to lowest emitting state of the acceptor unit that is formed by direct excitation as well as by an energy transfer process from excited donor unit accordingly to emission results. On the other hand, the attribution of the short-lived component of the transient absorption is not straightforward.[59] The spectrum of the short component (see inset of Figure 6), obtained by subtraction of the trace measured at 300 ns delay time (with the appropriate correction for the decrease of the signal due to the decay) from the initial trace, exhibits a broad absorption with a maximum around at 550 nm. In order to get more insight into the nature of this transient, laser flash photolysis experiments were also performed at 532 nm, where light selectively excites the acceptor unit. Very similar time dependent spectral changes were obtained (Figure S10 of Supporting Information) clearly indicating that the donor unit is not responsible for the short-lived transient.[60] We tentatively attribute the short-lived transient to a low-lying LC triplet state localized on the acceptor bridging ligand moiety, which decays by conversion to the MLCT triplet of the acceptor. The low energy position of such a state is consistent with the high degree of conjugation typical of phenyl-ethynylene-substituted bipyridine ligands.[61] Its nonemissive behavior (no transient with 100 ns lifetime is detected in time-resolved emission experiments) is consistent with the LC nature and short lifetime. The fact that this transient is not observed in the laser photolysis of $[Ir(dbpz)_2(bpy')]^+$ simply shows that this molecule, which lacks a substantial fragment (ethynyl-phenyl) of the bridging ligand moiety, is not a fully appropriate model. Upon excitation of the bichromophoric complex at 532 nm, the bridging-ligand localized LC triplet is assumed to be directly populated, in competition with the MLCT triplet, by intersystem crossing from the MLCT singlet manifold. Upon excitation at 355 nm,

dx.doi.org/10.1021/ic302222q | Inorg. Chem. 2013, 52, 2918−2926

where both the donor and acceptor units absorb, it could be in principle populated either by direct absorption of the acceptor or by energy transfer from the donor in a time scale (ns)

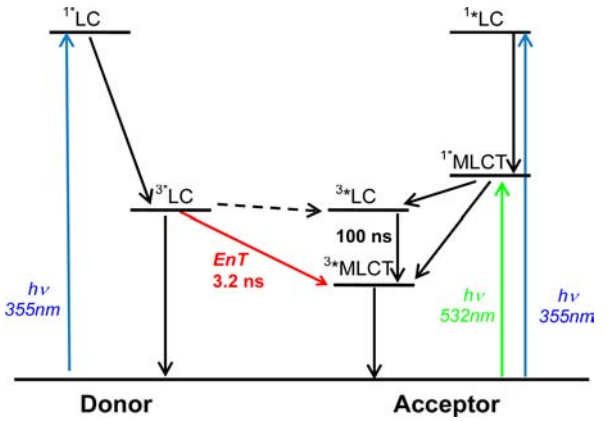

Figure 7. Schematic energy-level diagram and photophysical processes taking place in $[Ir(dfppy)_2$-Carbo-$Ir(dbpz)_2]^{2+}$ bichromophoric complex.

shorter than that of the experiment (8 ns). A schematic representation of the processes that occur upon laser excitation of the bichromophoric complex is reported in Figure 7.

CONCLUSION

We succeed in the synthesis of a multichromophoric Ir(III) complexes in which two disparate Ir fragments of different energy are linked by an inert and transparent para-closo carborane spacer. The logical construction of the mixed complex is controlled by a stepwise approach in which a first bipyidine subunit is connected via classical Pd(0) promoted cross-coupling reaction. This first unit is complexed to the "Ir(dfppy)" fragment, and the ancilliary alkyne function on the opposite side of the mononuclear complex is deprotected and cross-linked to the "Ir(dbpz)(bpyBr)" complex via a synthesis on the complex protocol. All complexes are redox active in the cathodic region, and the complex dbpz ligand is easier to reduce than the bpy ligand by ca. 160 mV, itself being easier to reduce than the dfppy ligand by ca. 630 mV. Altogether the results of transient experiments in emission as well in absorption give strong evidence for occurrence of an energy transfer process from donor to the acceptor unit. This process, faster than the laser pulse (8 ns), takes place in 3.2 ns that corresponds to a rate constant of 3.3×10^8 s^{-1}. The relatively slow rate for this process seems to confirm the absence of extensive electronic delocalization across the bridging ligand, although appropriate comparisons are not feasible because of the lack in the literature of similar systems containing the *p*-carborane spacer. A *p*-carborane-bridged Ru(II) binuclear complex was previously characterized.[44] In the mixed-valence Ru(II)−Ru(III) species an electron transfer process was observed with a slow rate constant (3.2×10^8 s^{-1}), clearly indicating low electronic conducting ability of the *p*-carborane unit.

ASSOCIATED CONTENT

Supporting Information

General methods, traces for NMR spectra, excitation spectrum of $[Ir(dfppy)_2$-Carbo-$Ir(dbpz)_2]^{2+}$, emission decay of the $[Ir(dfppy)_2$-Carbo-$Ir(dbpz)_2]^{2+}$, and transient absorption spectra of $[Ir(dfppy)_2$-Carbo-$Ir(dbpz)_2]^{2+}$. This material is available free of charge via the Internet at http://pubs.acs.org.

AUTHOR INFORMATION

Corresponding Author

*E-mail: idm@unife.it (M.T.I.); ziessel@unistra.fr (R.Z.).

Notes

The authors declare no competing financial interest.

ACKNOWLEDGMENTS

We thank the Centre National de la Recherche Scientifique (CNRS) for financial support of this work. M.T.I. thanks R. Argazzi for the 77 K emission measurements and F. Scandola for fruitful discussions.

REFERENCES

(1) (a) Balzani, V.; Credi, A.; Venturi, M. *ChemSusChem* **2008**, *1*, 26−58. (b) Harriman, A.; Ziessel, R. *Coord. Chem. Rev.* **1998**, *171*, 331−339.

(2) (a) Castellano, F. N.; Pomestchenko, I. E.; Shikhova, E.; Hua, F.; Muro, M. L.; Rajapakse, N. *Coord. Chem. Rev.* **2006**, *250*, 1819−1828. (b) Williams, J. A. G. *Top. Curr. Chem.* **2007**, *281*, 205−268. (c) Wong, K. M. C.; Yam, V. W. W. *Coord. Chem. Rev.* **2007**, *251*, 2477−2488. (d) Muro, M. L.; Rachford, A. A.; Wang, X. H.; Castellano, F. N. Platinum(II) Acetylide Photophysics. In *Photophysics of Organometallics*; Lees, A. J., Ed.; Springer-Verlag: Berlin, 2010; pp 159−191. (e) Kalinowski, J.; Fattori, V.; Cocchi, M.; Williams, J. A. G. *Coord. Chem. Rev.* **2011**, *255*, 2401−2425. (f) Ziessel, R.; Harriman, A. *Chem. Commun.* **2011**, *47*, 611−631.

(3) Ziessel, R.; De Nicola, A. *C. R. Chim.* **2009**, *12*, 450−478.

(4) (a) Hasobe, T. *Phys. Chem. Chem. Phys.* **2010**, *12*, 44−57. (b) Ward, M. D.; Barigelletti, F. *Coord. Chem. Rev.* **2001**, *216*, 127−154.

(5) (a) Diring, S.; Puntoriero, F.; Nastasi, F.; Campagna, S.; Ziessel, R. *J. Am. Chem. Soc.* **2009**, *131*, 6108−6110. (b) Ventura, B.; Barbieri, A.; Barigelletti, F.; Diring, S.; Ziessel, R. *Inorg. Chem.* **2010**, *49*, 8333−8346. (c) Diring, S.; Ziessel, R.; Barigelletti, F.; Barbieri, A.; Ventura, B. *Chem.—Eur. J.* **2010**, *16*, 9226−9236.

(6) Balzani, V.; Juris, A.; Venturi, M.; Campagna, S.; Serroni, S. *Chem. Rev.* **1996**, *96*, 759−833.

(7) (a) Balzani, V.; Bergamini, G.; Campagna, S.; Puntoriero, F. *Top. Curr. Chem.* **2007**, *280*, 1−36. (b) De Cola, L.; Belser, P. *Coord. Chem. Rev.* **1998**, *177*, 301−346. (c) Balzani, V.; Barigelletti, F.; De Cola, L. *Top. Curr. Chem.* **1990**, *158*, 31−71.

(8) (a) Balzani, V.; Scandola, F. *Supramolecular Chemistry: Concepts and Perspectives*; Horwood: Chichester, U.K., 1991. (b) Scandola, F. Molecular Wires. In *Encyclopedia of Supramolecular Chemistry*; Taylor & Francis: New York, 2007; pp 925−930.

(9) *Electron Transfer in Chemistry*; Balzani, V., Ed.; Wiley-VCH, Weinheim, 2001.

(10) (a) Amadelli, R.; Argazzi, R.; Bignozzi, C. A.; Scandola, F. *J. Am. Chem. Soc.* **1990**, *112*, 7099. (b) Dandliker, P. J.; Holmlin, R. E.; Barton, J. K. *Science* **1997**, *275*, 1465. Kelley, S. O.; Jackson, N. M.; Hill, M. G.; Barton, J. K. *Angew. Chem., Int. Ed.* **1999**, *38*, 941. (c) Harriman, A. *Angew. Chem., Int. Ed.* **1999**, *38*, 945. (d) Winkler, J. R.; Gray, H. B. *Chem. Rev.* **1992**, *92*, 369. (e) McLendon, G.; Hake, R. *Chem. Rev.* **1992**, *92*, 481. (f) Closs, G. L.; Miller, J. R. *Science* **1988**, *240*, 440. (g) Paddon-Row, M. N. *Acc. Chem. Res.* **1994**, *27*, 18. (h) Klan, P.; Wagner, P. J. *J. Am. Chem. Soc.* **1998**, *120*, 2198.

(11) Molecular Wires. *Topics in Current Chemistry*; De Cola, L., Ed.; Springer: New York, 2005; p 257.

(12) Davis, W. B.; Svec, W. A.; Ratner, M. A.; Wasielewski, M. R. *Nature* **1998**, *396*, 60.

(13) Effenberger, F.; Wolf, H. C. *New J. Chem.* **1991**, *15*, 117.

(14) Pickaert, G.; Ziessel, R. *Tetrahedron Lett.* **1998**, *39*, 3497.

(15) Wagner, R. W.; Lindsey, J. S.; Seth, J.; Palaniappan, V.; Bocian, D. F. *J. Am. Chem. Soc.* **1996**, *118*, 3996.

(16) Harriman, A.; Ziessel, R. *Platinum Met. Rev.* **1996**, *40*, 26; **1996**, *40*, 72.

(17) (a) Tzalis, D.; Tor, Y. *Chem. Commun* **1996**, 1043. Tzalis, D.; Tor, Y. *J. Am. Chem. Soc.* **1997**, *119*, 852. (b) Connors, P. J., Jr.; Tzalis, D.; Dunnick, A. L.; Tor, Y. *Inorg. Chem.* **1998**, *37*, 1121.
(18) Schermann, G.; Grösser, T.; Hampel, F.; Hirsch, A. *Chem.—Eur. J.* **1997**, *3*, 1105.
(19) Siemeling, U.; Vorfeld, U.; Neumann, B.; Stammler, H.-G.; Zanello, P.; Fabrizi de Biani, F. *Eur. J. Inorg. Chem.* **1999**, 1.
(20) Kim, Y.; Lieber, C. M. *Inorg. Chem.* **1989**, *28*, 3990.
(21) Sauvage, J.-P.; Collin, J.-P.; Chambron, J.-C.; Guillerez, S.; Coudret, C.; Balzani, V.; Barigelletti, F.; De Cola, L.; Flamigni, L. *Chem. Rev.* **1994**, *94*, 993.
(22) Schlicke, B.; Belser, P.; De Cola, L.; Sabbioni, E.; Balzani, V. *J. Am. Chem. Soc.* **1999**, *121*, 4207.
(23) (a) Indelli, M. T.; Chiorboli, C.; Flamigni, L.; De Cola, L.; Scandola, F. *Inorg. Chem* **2007**, *46*, 5630−5641. (b) Indelli, M. T.; Orlandi, M.; Chiorboli, C.; Ravaglia, M.; Scandola, F.; Lafolet, F.; Welter, S.; De Cola, L. *J. Phys. Chem. A* **2012**, *116*, 119−131.
(24) Wenger, O. S. *Chem. Soc.Rev.* **2011**, *40*, 3538−3550.
(25) Grubbs, R. H.; Kratz, D. *Chem. Ber.* **1993**, *126*, 149.
(26) (a) Jones, L., II; Schumm, J. S.; Tour, J. M. *J. Org. Chem.* **1997**, *62*, 1388. (b) Huang, S.; Tour, J. M. *Tetrahedron Lett.* **1999**, *40*, 3347.
(27) Pearson, D. L.; Tour, J. M. *J. Org. Chem.* **1997**, *62*, 1376.
(28) Vollmer, M. S.; Würthner, F.; Effenberger, F.; Emele, P.; Meyer, D. U.; Stümpfig, T.; Port, H.; Wolf, H. C. *Chem.—Eur. J.* **1998**, *4*, 260.
(29) Jousselme, B.; Blanchard, P.; Oçafrain, M.; Allain, M.; Levillain, E.; Roncali, J. *J. Mater. Chem.* **2004**, *14*, 421.
(30) Barbieri, A.; Ventura, B.; Ziessel, R. *Cood. Chem. Rev.* **2012**, *256*, 1732−1741.
(31) (a) Barigelletti, F.; Flamigni, L. *Chem. Soc. Rev.* **2000**, *29*, 1−12. (b) Albinsson, B.; Martensson, J. *Phys. Chem. Chem. Phys.* **2010**, *12*, 7338−7351.
(32) Wenger, O. S. *Acc. Chem. Res.* **2011**, *44*, 25−35.
(33) Ziessel, R.; Bäuerle, P.; Ammann, M.; Barbieri, A.; Barigelletti, F. *Chem. Commun.* **2005**, 802−804.
(34) (a) Kaszynski, P.; Pakhomov, S.; Tesh, K. F.; Young, V. G., Jr. *Inorg. Chem.* **2001**, *40*, 6622−6631. (b) Kaszynski, P.; Douglass, A. G. *J. Organomet. Chem.* **1999**, *581*, 28−38.
(35) Fox, M. A.; Wade, K. *J. Mater. Chem.* **2002**, *12*, 1301−1306.
(36) (a) Taylor, J.; Cruso, J.; Newlon, A.; English, U.; Ruhlandt-Senge, K.; Spencer, J. T. *Inorg. Chem.* **2001**, *40*, 3381−3388. (b) Allis, D. G.; Spencer, J. T. *Inorg. Chem.* **2001**, *40*, 3373−3380.
(37) Vicente, J.; Chicote, M.-T.; Alvarez-Falcon, M. M. *Organometallics* **2003**, *22*, 4792−4797 and references therein.
(38) Jude, H.; Disteldorf, H.; Fischer, S.; Wedge, T.; Hawkridge, A. M.; Arif, A. M.; Hawthorne, M. F.; Muddiman, D. C.; Stang, P. J. *J. Am. Chem. Soc.* **2005**, *127*, 12131−12139.
(39) Zheng, Z.; Knobler, C. B.; Mortimer, M. D.; Kong, G.; Hawthorne, M. F. *Inorg. Chem.* **1996**, *35*, 1235−1243.
(40) (a) Corsini, M.; Fabrizi de Biani, F.; Zanello, P. *Coord. Chem. Rev.* **2006**, *250*, 1351−1372. (b) Hosmane, N. S.; Maguire, J. A. *Eur. J. Inorg. Chem.* **2003**, 3989−3999.
(41) (a) Soloway, A. H.; Tjarks, W.; Barnum, B. A.; Rong, F.-G.; Barth, R. F.; Codogni, I. M.; Wilson, J. G. *Chem. Rev.* **1998**, *98*, 1515−1562. (b) Hawthorne, M. F.; Maderna, A. *Chem. Rev.* **1999**, *99*, 3421−3434.
(42) (a) Bregadze, V. I. *Chem. Rev.* **1992**, *92*, 209−223. (b) Williams, R. E. *Chem. Rev.* **1992**, *92*, 177−207. (c) Plesek, J. *Chem. Rev.* **1992**, *92*, 269−278. (d) Leites, L. A. *Chem. Rev.* **1992**, *92*, 279−323. (e) Schwab, P. F. H.; Levin, M. D.; Michl, J. *Chem. Rev.* **1999**, *99*, 1863−1933.
(43) Ziessel, R.; Ulrich, G.; Olivier, J .-H.; Bura, T.; Sutter, A. *Chem. Commun.* **2010**, *46*, 7978−7980.
(44) Ghirotti, M.; Schwab, P.; Indelli, M. T.; Chiorboli, C.; Scandola, F. *Inorg. Chem.* **2006**, *45*, 4331−4333.
(45) Hablot, D.; Sutter, A.; Retailleau, P.; Ziessel, R. *Chem.—Eur. J.* **2012**, *18*, 1890−1895.
(46) Grosshenny, V.; Romero, F. M.; Ziessel, R. *J. Org. Chem.* **1997**, *62*, 1491−1500.
(47) Romero, F. M.; Ziessel, R. *Tetrahedron Lett.* **1995**, *36*, 6471−6474.
(48) (a) Sprouse, S.; King, K. A.; Spellane, P. J.; Watts, R. J. *J. Am. Chem. Soc.* **1984**, *106*, 6647−6653. (b) Coppo, P.; Edward A. Plummer, E. A.; De Cola, L. *Chem. Commun.* **2004**, 1744−1775.
(49) Hideo, K. "*Iridium Complex and Luminescent Materials*" JP2005298483, A 20051027.
(50) Flamigni, F.; Barbieri, A.; Sabatini, C.; Ventura, B. *Top. Curr. Chem.* **2007**, *281*, 143−203.
(51) Plummer, E. A.; Hofstraat, J. W.; De Cola, L. *Dalton Trans.* **2003**, 2080−2084.
(52) Care must be taken in the case of iridium cyclometalated in the use of localized descriptions of molecular orbitals and transitions, as the HOMO orbitals may be significantly delocalized over the cyclometalating phenyls. In fact, for several of such systems, mixed descriptions seem to be more appropriate.[7]
(53) Polson, M.; Fracasso, S.; Bertolasi, V.; Ravaglia, M.; Scandola, F. *Inorg. Chem* **2004**, *43*, 1950−1956 (also see ref 7).
(54) Even though the emission bands of the two chromophoric units show very little overlap (Figure 3), the difference in radiative rate constants (Table 2) makes the acceptor emission non-negligible in these experiments.
(55) (a) Förster, T. *Ann. Phys.* **1948**, *2*, 55. (b) Förster, T. *Discuss. Faraday Soc.* **1959**, *27*, 7−17.
(56) Du, H.; Fuh, R. A.; Li, J.; Corkan, A.; Lindsey, J. S. *Photochem. Photobiol.* **1998**, *68*, 141−142.
(57) Dexter, D. L. *J. Chem. Phys.* **1953**, *21*, 836.
(58) Braterman, P. S.; Harriman, A.; Heath, G. A.; Yellowlees, L. J. *J. Chem. Soc., Dalton Trans.* **1983**, 1801.
(59) It can be stressed that the presence of an impurity was excluded by characterization techniques that ensured the high purity of the sample.
(60) Flash photolysis experiments were also performed in MeOH and in CH_3CN solutions, but no solvent effects were observed.
(61) Birckner, E.; Grummt, U.-W.; Goller, A. H.; Pautzsch, T.; Egbe, D. A. M.; Al-Higari, M.; Klemm, E. *J. Phys. Chem. A* **2001**, *105*, 10307−10315.